

## Particle Decays

### 15.1 Introduction

In this chapter we discuss experiments where the run architecture is significantly different from that of standard *in-out* experiments such as particle scattering. We apply the quantized detector network (QDN) formalism to particle decays, the ammonium molecular system, Kaon-type regeneration decay experiments, and quantum Zeno experiments. In all of these experiments, the problem is the modeling of time, which conventionally is taken to be continuous. In QDN, time is treated in terms of stages, which are discrete. We show how the QDN formalism deals with such experiments.

In standard quantum mechanics (QM), time is assumed to be continuous. That is a legacy from classical mechanics (CM), which does not concern itself in general with the processes of observation. CM assumes systems under observation (SUOs) “have” physical properties that are independent of how they are observed. In contrast, QM cannot be considered without a discussion of the processes of observation. On close inspection of any process of observation, *as it is actually carried out in the laboratory and not how it is modeled theoretically*, the continuity of time does not look quite so obvious.

The problem is that there are two mutually exclusive views about the nature of observation in physics. These were discussed in detail by Misra and Sudarshan (MS) in an influential paper on the quantum Zeno effect (Misra and Sudarshan, 1977). On the one hand, no known principle forbids the continuity of time, so the axioms of QM are stated implicitly in terms of continuous time. When the Schrödinger equation is postulated to be one of them (Peres, 1995), temporal continuity is assumed explicitly. On the other hand, it is an empirical fact that no experiment can actually monitor any SUO in a truly continuous way. All references to continuous time measurements are invariably based on statistical modeling of complex processes, with the continuity of time having much the same status as that of temperature. Such effective parameters are extremely useful in

physics, but their status as model-dependent, emergent attributes of SUOs, and the apparatus used to observe them, should always be kept in mind.

The best that could be done toward simulating temporal continuity in physics would be to perform a sequence of experiments with a carefully prescribed decreasing measurement time scale, such as occurs in experiments investigating the phenomenon known as the quantum Zeno effect (Itano et al., 1990).

MS analyzed particle decay processes and asked certain questions about them not normally investigated in quantum mechanics. Three of these questions were referred to as  $P$ ,  $Q$ , and  $R$  and this convention will be followed here.

### $P(t|\Psi)$

This question asks for the probability that an unstable system prepared at time zero in state  $\Psi$  has decayed sometime during the interval  $[0, t]$ .

### $Q(t|\Psi)$

This question asks for the probability that the prepared state has *not* decayed during this interval.

### $R(t_1, t|\Psi)$

This question asks for the probability that the state has not decayed during the interval  $[0, t_1]$ , where  $0 < t_1 < t$ , and has decayed during the interval  $[t_1, t]$ .

Here we come across an example where mathematics and logic cannot be used to explore physics. We pointed out in Section 2.10 that the validation<sup>1</sup> of the negation  $\neg P$  of a physical proposition  $P$  cannot always be undertaken by the same apparatus that is used to validate  $P$ . The point is that suppose we had used apparatus  $A_P$  to answer MS's question  $P(t|\Psi)$  by looking for decay products of an unstable SUO and had found no such decay products over any given interval of time. We could not conclude that the SUO was absolutely stable; there could be decay products that our apparatus could not detect. At best we could only say that the SUO was stable *relative* to  $A_P$ .

In physics, therefore, we cannot simply assert  $Q(t|\Psi) = 1 - P(t|\Psi)$  as an empirical fact, because as we stated in Chapter 2, what are important in physics are generalized propositions, and these require full specification of apparatus. In order to answer  $Q(t|\Psi)$ , we would have to use apparatus  $A_Q$ , which could be very different from  $A_P$ .

Likewise, in order to answer MS's question  $R(t_1, t|\Psi)$ , we would have to use apparatus  $A_R$ .

The point made by MS is not quite the same as what we have just made. Our concern is about apparatus, theirs was about time. MS stressed that  $P(t|\Psi)$ ,  $Q(t|\Psi)$ , and  $R(t_1, t|\Psi)$  are not what quantum mechanics normally calculates,

<sup>1</sup> Our convention is that *validation* means the *attempt* to establish the truth of a proposition.

which is the probability distribution of the time at which decay occurs, denoted by  $T$ . The difference as they saw it is that the  $P$ ,  $Q$ , and  $R$  questions involve a continuous set of observations (according to the standard paradigm), or the nearest practical equivalent of it, during each run of the experiment, whereas  $T$  involves a set of repeated runs, each with a one-off observation at a different time to determine whether the particle has decayed or not by that time. Because  $P$ ,  $Q$ , and  $R$  involve an experimental architecture different from  $T$ , it should be expected that empirical differences might be observed.

Note that the observations referred to by MS to can have negative outcomes; i.e., a failure to detect an expected particle decay in an experiments counts as an observation. The correct statement of such an observation is not that the particle is stable, but that that particular experiment has failed to detect any decay.

MS emphasized the limitations of QM, stressing that although it works excellently in many situations, QM does not readily give a complete picture of experiments probing questions such as  $P$ ,  $Q$ , and  $R$ . They concluded that “there is no standard and detailed theory for the actual coupling between quantum systems and the *classical measuring apparatus*” (Misra and Sudarshan, 1977). We fully agree. QDN is a relatively simplified attempt to move toward such a theory.

Our first task in this chapter is to apply QDN to the simplest idealized decay process, a particle decaying via a single channel. The quantum Zeno effect is then discussed. That effect demonstrates that the answer as to whether a system decays while it is being monitored or whether it remains in its initial state depends on the experimental context, i.e., the details of the apparatus and the measurement protocol involved. We follow this by applying QDN to more complex phenomena such as the ammonium molecule and neutral Kaon decay. We show how QDN can readily provide the empirical architecture to describe the spectacular phenomenon of Kaon decay regeneration, originally discussed by Gell-Mann and Pais in standard QM (Gell-Mann and Pais, 1955).

It will be shown that for all of these phenomena, QDN incorporates probability conservation at all levels of the discussion and therefore does not require the introduction of any ad hoc imaginary terms in any energies or the use of non-Hermitian Hamiltonians.

## 15.2 One Species Decays

In this subsection, we apply QDN to the description of what in standard terminology would be called the decay of an unstable particle, the initial state  $X$  of which can decay into some multiparticle state  $Y$ . Our aim is to show that the QDN account of such processes readily conserves total probability at all stages. Because the essence of such processes lies in the temporal architecture, the momenta and other attributes of the particles involved will be ignored here, the discussion being designed to illuminate the basic principles of the formalism

only. Should such aspects be required, the formalism can readily deal with them by introducing an “internal” Hilbert space associated with the SUO states.

The run architecture follows the pattern used throughout this book, with labstate preparation for each run being completed by an initial stage denoted as  $\Sigma_0$ , and referred to as stage zero. All subsequent stages in that run are counted from stage zero, so  $\Sigma_1$  is the first stage (after stage zero).

By stage  $\Sigma_0$  of any given run, the observer will have contextual evidence that they have prepared an  $X$ -particle state, in the language of standard QM. This is represented in QDN by the normalized labstate  $\Psi_0 \equiv \widehat{\mathbb{A}}_0^X \mathbf{0}_0$ , which we have previously designated a *preparation switch*.

Now consider the first stage,  $\Sigma_1$ , at which the observer has the means to detect any decay. Suppose by that stage, the labstate is now represented by  $\Psi_1$  and given by

$$\Psi_1 \equiv \mathbb{U}_{1,0} \Psi_0 = (\alpha \widehat{\mathbb{A}}_1^X + \beta \widehat{\mathbb{A}}_1^Y) \mathbf{0}_1, \quad |\alpha|^2 + |\beta|^2 = 1. \quad (15.1)$$

Here the first term on the right-hand side (RHS) represents the possibility that the particle has *not* decayed, whereas the second term, involving  $Y$ , represents the possibility that a decay has occurred.

It is part of the underlying philosophy of QDN that the term in  $Y$  in Eq. (15.1) does not model specific details of the  $Y$  state. It models a *yes/no* possibility that something has happened. It is an example of a virtual detector rather than a real detector. A virtual detector is informational in character, not necessarily directly identifiable with a specific, real detector in the laboratory, although such things are necessary to establish the context for the labstate  $Y$ .

To clarify this point further, suppose that the multiparticle state  $Y$  consisted of  $N$  identifiable particles. We have *not* modeled here the stage  $\Sigma_1$  labstate by a term in (15.1) such as  $\beta \widehat{\mathbb{A}}_1^{Y^1} \widehat{\mathbb{A}}_1^{Y^2} \widehat{\mathbb{A}}_1^{Y^3} \dots \widehat{\mathbb{A}}_1^{Y^N} \mathbf{0}_1$ , where for example  $\widehat{\mathbb{A}}_1^{Y^i}$  would create a signal in a specific detector for decay component particle  $Y^i$  at stage  $\Sigma_1$ . We could do that, if we wanted to, however. That would undoubtedly add to the complexity of a problem that already has some degree of complexity in its architecture, so that is a scenario where a computer algebra approach to QDN would be most suitable.

The modeling of the labstate  $\Psi_1$  given by (15.1) does however include some desirable features that we have put in “by hand.” We exclude from the RHS of (15.1) the possibility that we find no signals whatsoever at stage  $\Sigma_1$ ; that is, we exclude the signal ground state  $\mathbf{0}_1$ . This means that the apparatus is what we have referred to before as *calibrated*.

In the same spirit, we exclude the signality-two state  $\widehat{\mathbb{A}}_1^X \widehat{\mathbb{A}}_1^Y \mathbf{0}_1$ , on the grounds that any run with a labstate consisting of the original particle *and* its decay product would be discounted by the observer as contaminated by external influences (as happens in real experiments).

From (15.1), the amplitude  $\mathcal{A}(X_1|X_0)$  for the particle *not* to have decayed by stage  $\Sigma_1$  is given by

$$\mathcal{A}(X_1|X_0) \equiv \overline{\mathbf{0}}_1 \mathbb{A}_1^X \Psi_1 = \alpha, \tag{15.2}$$

while the amplitude  $\mathcal{A}(Y_1|X_0)$  for the particle to have made the transition to state  $Y$  by stage  $\Sigma_1$  is given by

$$\mathcal{A}(Y_1|X_0) \equiv \overline{\mathbf{0}}_1 \mathbb{A}_1^{Y_1} \Psi_1 = \beta. \tag{15.3}$$

Here we have used the fact that  $[\widehat{\mathbb{A}}_n^X, \mathbb{A}_n^Y] = 0$ , and so on.

From the above, we see that

$$|\mathcal{A}(X_1|X_0)|^2 + |\mathcal{A}(Y_1|X_0)|^2 = 1, \tag{15.4}$$

so total probability is conserved.

The above probabilities can also be calculated directly as expectation values of partial questions. For the probability  $\Pr(X_1|X_0)$  of no decay by stage  $\Sigma_1$ , we find  $\Pr(X_1|X_0) \equiv \overline{\Psi}_1 \widehat{\mathbb{P}}_1^X \Psi_1 = |\alpha|^2$ , while the probability  $\Pr(Y_1|X_0)$  of decay into  $Y$  by stage  $\Sigma_1$  is given by  $\Pr(Y_1|X_0) \equiv \overline{\Psi}_1 \widehat{\mathbb{P}}_1^{Y_1} \Psi_1 = |\beta|^2$ . Note that these are contextual probabilities: we noted at the previous section that these are statements valid only relative to the detectors used, which are assumed suitable for what they are supposed to detect.

On the RHS of (15.3), the label is  $Y_1$ ; that is, the decay state label is itself labeled by a temporal subscript, in this case the number 1, which is the stage  $\Sigma_1$  at which the amplitude is calculated for. This label of a label is significant. It registers the fact that when a detector is triggered, it does so irreversibly. The stage at which this happens is a crucial feature of the analysis, being directly related to the measurement issues discussed by MS (Misra and Sudarshan, 1977). Our architecture is based on monitoring the state of the SUO as much as possible, that is, attempting to perform as good an approximation to continuous-in-time monitoring as our equipment allows.

The above process conserves signality one, so the dynamics can be discussed economically in terms of the evolution of the signal operators rather than the labstates. For instance, evolution from stage  $\Sigma_0$  to stage  $\Sigma_1$  can be given in the form

$$\widehat{\mathbb{A}}_0^X \rightarrow \mathbb{U}_{1,0} \widehat{\mathbb{A}}_0^X \overline{\mathbb{U}}_{1,0} = \alpha \widehat{\mathbb{A}}_1^X + \beta \widehat{\mathbb{A}}_1^{Y_1}, \tag{15.5}$$

where  $\mathbb{U}_{1,0}$  is a semi-unitary operator satisfying the rule  $\overline{\mathbb{U}}_{1,0} \mathbb{U}_{1,0} = \mathbb{I}_0$ , with  $\mathbb{I}_0$  being the identity for the initial lab register  $\mathcal{Q}_0 \equiv \mathcal{Q}_0^X$  and  $\overline{\mathbb{U}}_{1,0}$  being the retraction of  $\mathbb{U}_{1,0}$ .

Process (15.5) involves a change in rank, since  $\mathcal{Q}_1 \equiv \mathcal{Q}_1^X \mathcal{Q}_1^{Y_1}$ , but not in signality. Because  $\dim \mathcal{Q}_1 > \dim \mathcal{Q}_0$ , the evolution operator is properly semi-unitary, that is, satisfies the condition  $\mathbb{U}_{1,0} \overline{\mathbb{U}}_{1,0} \neq \mathbb{I}_1$ , which is a statement of irreversibility relative to the observer. This is a critical feature of the experiments discussed in this chapter, apart for the ammonium molecule, and is the reason for the apparent loss of probability in conventional Schrödinger wave mechanics descriptions of unstable particles. In those descriptions, a common strategy is to consider only the Hilbert space of the original SUO and add an imaginary

term  $-i\Gamma$  to energies, thereby forcing wave functions to fall off with time, with the interpretation that this represents particle decay. Where this probability loss goes is left unstated.

In relativistic quantum field theory, such as quantum electrodynamics (QED), the architecture is usually different. There, the Hilbert space is big enough to accommodate particles (such as muons) and their decay products. Decays are treated as scattering problems, with initial undecayed particles coming in at remote negative (infinite past) time and decay products going out at remote positive (infinite future) time. The extraction of decay lifetimes then is usually done in a heuristic manner, usually involving manipulation with symbols that are nominally divergent, such as dividing an amplitude by the four-volume measure of Minkowski spacetime in order to determine a flux decay rate. Our ambition in QDN is to avoid such manipulations while retaining probability conservation.

The QDN description of the next stage of the process, from stage  $\Sigma_1$  to stage  $\Sigma_2$ , is more subtle and involves a *null test*. Considering the labstate of the above decay process at stage  $\Sigma_1$ , there are now two terms to consider.

### No Decay

The first term on the RHS in (15.1),  $\alpha\widehat{\mathbb{A}}_1^X\mathbf{0}_1$ , corresponds to a *no decay* outcome by stage  $\Sigma_1$ . This potential outcome can now be regarded as a preparation, at stage  $\Sigma_1$ , of an initial  $X$  state that could subsequently decay into a  $Y$  state or not, with the same dynamical characteristics as for the first temporal link of the run, held between stages  $\Sigma_0$  and  $\Sigma_1$ . If the measured laboratory time interval  $\tau_{10} \equiv t_1 - t_0$  between stages  $\Sigma_0$  and  $\Sigma_1$  is the same, within experimental uncertainty, as the measured laboratory time interval  $\tau_{21} \equiv t_2 - t_1$  between stages  $\Sigma_1$  and  $\Sigma_2$ , and so on for subsequent links, then spatial and temporal homogeneity may be assumed, if the apparatus has been set up in the laboratory carefully enough. This will be a physically reasonable assumption in the absence of gravitational fields and in the presence of suitable apparatus.

### Decay

The second term,  $\beta\widehat{\mathbb{A}}_1^{Y_1}\mathbf{0}_1$ , in (15.1) corresponds to *decay having occurred during the first time interval*. Such an outcome is irreversible in this example, but this is not an inevitable assumption in general. Situations where the  $Y$  state could revert back to the  $X$  state are more complicated but of empirical interest, such as in the ammonium maser and Kaon and B meson decay. These scenarios are discussed later sections in this chapter.

Assuming homogeneity, the next stage of the evolution is given by

$$\widehat{\mathbb{A}}_1^X \rightarrow \mathbb{U}_{2,1}\widehat{\mathbb{A}}_1^X \overline{\mathbb{U}}_{2,1} = \alpha\widehat{\mathbb{A}}_2^X + \beta\widehat{\mathbb{A}}_2^{Y_2}, \quad (15.6)$$

$$\widehat{\mathbb{A}}_1^{Y_1} \rightarrow \mathbb{U}_{2,1}\widehat{\mathbb{A}}_1^{Y_1} \overline{\mathbb{U}}_{2,1} = \widehat{\mathbb{A}}_2^{Y_1}. \quad (15.7)$$

Equation (15.7) is justified as follows. The decay term in (15.1), proportional to  $\widehat{\mathbb{A}}_1^{Y_1}$  at stage  $\Sigma_1$ , corresponds to the possibility of detecting a decay product

state  $Y$  at that time. Now there is nothing that requires this information to be extracted precisely at that stage. The experimentalist could choose, or indeed be required, to delay information extraction until some later stage, effectively placing the decay product observation “on hold.” The inherent irreversibility of signal detectors means that, as a rule, such signals on hold are not lost.

As stated above, this may be represented in QM by passing a state through a null test, which does not alter it. In QDN this is represented by Eq. (15.7). Essentially, quantum information about a decay is isolated from the rest of the experiment and passed forward in time until it is physically extracted.

The lab register  $\mathcal{Q}_2$  at stage  $\Sigma_2$  has rank three, being the tensor product  $\mathcal{Q}_2 \equiv Q_2^X Q_2^{Y_1} Q_2^{Y_2}$ . Semi-unitary evolution from stage  $\Sigma_0$  to stage  $\Sigma_2$  is still of signality one and is given by

$$\hat{A}_0^X \rightarrow \mathbb{U}_{2,1} \mathbb{U}_{1,0} \hat{A}_0^X \bar{\mathbb{U}}_{1,0} \bar{\mathbb{U}}_{2,1} = \alpha^2 \hat{A}_2^X + \alpha \beta \hat{A}_2^{Y_2} + \beta \hat{A}_2^{Y_1}, \quad (15.8)$$

with the various probabilities being read off as the squared moduli of the corresponding terms.

The temporal architecture of this process is given in Figure 15.1. It will be apparent from a close inspection of (15.8) that what appears to look like a space-time description with a specific arrow of time is being built up, with a memory of the change of rank of the lab register at stage  $\Sigma_1$  being propagated forward in time to stage  $\Sigma_2$ . This is represented by the contribution involving  $\hat{A}_2^{Y_1}$ , which is interpreted as a potential decay process that may have occurred by stage  $\Sigma_1$  and contributing to the overall labstate amplitude at stage  $\Sigma_2$ .

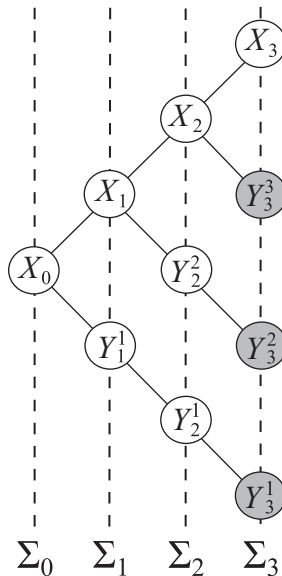


Figure 15.1. The temporal architecture of a single  $X$  particle decay experiment.

Subsequently the process continues in an analogous fashion, with the rank of the lab register increasing by one at each time step. By stage  $\Sigma_n$ , assuming homogeneity, the dynamics is given by

$$\widehat{\mathbb{A}}_0^X \rightarrow \mathbb{U}_{n,0} \widehat{\mathbb{A}}_0^X \overline{\mathbb{U}}_{n,0} = \alpha^n \widehat{\mathbb{A}}_n^X + \beta \sum_{i=1}^n \alpha^{i-1} \widehat{\mathbb{A}}_n^{Y_i}, \tag{15.9}$$

where  $\mathbb{U}_{n,0} \equiv \mathbb{U}_{n,n-1} \mathbb{U}_{n-1,n-2} \dots \mathbb{U}_{1,0}$  is semi-unitary and satisfies the constraint  $\overline{\mathbb{U}}_{n,0} \mathbb{U}_{n,0} = \mathbb{I}_0$ .

The amplitude  $\mathcal{A}(X, n|X, 0)$  that the original state has *not* decayed by stage  $\Sigma_n$  can be immediately read off the RHS of (15.9) and is given by

$$\mathcal{A}(X, n|X, 0) = \overline{\mathbf{0}}_n \mathbb{A}_n^X \mathbb{U}_{n,0} \widehat{\mathbb{A}}_0^X \mathbf{0}_0 = \alpha^n. \tag{15.10}$$

The probability  $\Pr(X, n|X, 0)$  of no decay by stage  $\Sigma_n$  is the squared modulus of this amplitude, so provided  $\beta \neq 0$ , this probability falls monotonically with increasing  $n$ , consistent with our expectations of particle decay. Specifically, if we write  $\alpha = e^{i\theta - \frac{1}{2}\Gamma\tau}$ , where  $\theta$  is some real phase,  $\Gamma$  is a characteristic lifetime associated with the decay, and  $\tau$  is the effective time between successive stages, then we have

$$\Pr(X, n|X, 0) = e^{-\Gamma n\tau}, \tag{15.11}$$

which is the exponential decay form expected with such phenomena.

**Commentary**

Figure 15.1 does not reveal the full complexity of what is going on. That will be appreciated by the observation that the labstate has signality one at every stage. This means that at any stage, either the original state has not decayed or it has decayed *once*, either at the stage being examined or prior to that stage.

This stage diagram reinforces the message that the Block Universe picture of reality is too simplistic, because that picture is a classical record of what was actually observed and cannot include the future of whatever “now” is being discussed (which is stage  $\Sigma_0$  here), unless the vacuous assumption is made that the future is single valued and predetermined. That would not be compatible with quantum principles as we know them, however. Figure 15.1 refers to the future of stage  $\Sigma_0$  and the probability outcomes predicted for the observer by QM, for that stage only; it is not a valid stage diagram for any process time stage after stage  $\Sigma_0$ . The contextuality of stage diagrams underlines the message that physics is contextual, never absolute.

**15.3 The Quantum Zeno Effect**

The discussion at this point calls for some care with limits, because there arises the theoretical possibility of encountering the so-called *quantum Zeno effect*, in which a carefully monitored state of an unstable SUO appears not to change.

In the following, we will assume that the parameter  $\alpha$  in the one-particle decay discussed above satisfies  $|\alpha| < 1$ , because the case  $|\alpha| = 1$  corresponds to a stable particle, which is of no interest here.

Consider the physics of particle decay. Calculated probabilities should be functions of labtime, the clock time used by the observer in the laboratory. Labtime is not assumed here to be a continuous variable on the microscopic level. Instead, it is linked to the scale of time associated with successive stages, and this is determined by the apparatus used. The temporal subscript  $n$  in our concept of stages will, when it is so arranged, correspond to a physical interval of time  $\tau$ , where  $\tau$  is some reasonably well-defined time scale characteristic of the apparatus.

*Certainly*, stages need not be strictly regulated in terms of being equally spaced out in time. But in the sort of experiments relevant to this chapter, there will be such an interval  $\tau$ , and it will be typically a minute fraction of a second, but certainly nowhere near the Planck time scale of  $10^{-44}$  second. Indeed, the conjecture that there is such a Planck time scale remains conjectural and has received some meaningful criticism (Meschini, 2007). The smallest interval currently that has been measured empirically is of the order  $10^{-23}$  second, which is on the shortest hadronic resonance scale, comparable with the time light takes to cross a proton diameter. More realistic measurement scales that could be involved in our discussion directly would probably be electromagnetic in origin, in the range of  $10^{-9}$  to  $10^{-18}$  second. For instance, the shortest controllable time is about 10 attoseconds, that is, about  $10^{-17}$  second (Koke et al., 2010). Experimentalists would generally have a good understanding of what their relevant  $\tau$  is.

Suppose first that we have some reason to believe that we can relate the transition amplitude  $\alpha$  to the characteristic time  $\tau$  by the rule  $|\alpha|^2 \equiv e^{-\Gamma\tau}$ , where  $\Gamma$  is a characteristic inverse time introduced to satisfy this relation. Then the survival probability  $P(t_n)$  is given by  $P(t) \equiv \Pr(X, n|X, 0) = e^{-\Gamma t}$ , which is the usual exponential decay formula. No imaginary term proportional to  $\Gamma$  in any supposed Hamiltonian or energy has been introduced in order to obtain exponential decay.

A subtlety may arise here, however. Exponential decay implies that  $|\alpha|^2$  is an analytic function of  $\tau$  with a Taylor expansion of the form

$$|\alpha|^2 = 1 - \Gamma\tau + O(\tau^2), \quad (15.12)$$

i.e., one with a nonzero linear term. Under such circumstances, the standard result  $\lim_{n \rightarrow \infty} (1 - x/n)^n = e^{-x}$  leads to the exponential decay law. The possibility remains, however, that the dynamics of the apparatus is such that the linear term in (15.12) is zero, so that the actual expansion is of the form

$$|\alpha|^2 = 1 - \gamma\tau^2 + O(\tau^3), \quad (15.13)$$

where  $\gamma$  is a positive constant (Itano et al., 1990). Then in the limit  $n \rightarrow \infty$ , where  $n\tau \equiv t$  is held fixed, the result is given by

$$\lim_{n \rightarrow \infty, n\tau=t \text{ fixed}} (1 - \gamma\tau^2 + O(\tau^3))^n = 1, \quad (15.14)$$

which gives rise to the quantum Zeno effect scenario. An expansion of the amplitude of the form  $a = 1 + i\mu\tau + \nu\tau^2 + O(\tau^3)$  is consistent with (15.13), for example, if  $\mu$  is real and  $\mu^2 + \nu + \nu^* < 0$ .

To understand properly what is going on, it is necessary to appreciate that there are two competing limits being considered: one where an SUO is being repeatedly observed over an increasingly large macroscopic laboratory time scale  $t \equiv n\tau$ , and another one where more and more observations are being taken in succession, each separated on a time scale  $\tau$  that is being brought as close to zero as possible by the experimentalist. In each case, the limit cannot be achieved in the laboratory. The result is that in such experiments, the specific properties of the apparatus and the experimental protocol may play a decisive role in determining the results. If the apparatus is such that (15.12) holds, then exponential decay will be observed, whereas if the apparatus behaves according to the rule (15.13), or any reasonable variant of it, then approximations to the quantum Zeno effect should be observed.

From the QDN perspective, the quantum Zeno effect can be understood from the architecture of decay observation as follows. Looking at Figure 15.1, we see that there is one channel, denoted by circles with an  $X$ , that runs across all stages. That channel is the “no decay” channel. If during a run involving a great number of stages the net probability of any of the other outcomes being detected is sufficiently low, then it would appear that the original system was stable. However, given enough stages with a fixed duration  $\tau$  between each, the decay outcomes would eventually win out. The quantum Zeno effect therefore relies on having as brief a duration  $\tau$  as possible and finding the critical time scale over which the apparent effect could be observed.

Another way of understanding the quantum Zeno effect is in terms of *environment*. For instance, a free neutron will decay with a mean lifetime of about 880 seconds, whereas inside a nucleus, neutrons are generally stable. We can understand the quantum Zeno effect as the effect of the detection environment on an otherwise unstable system.

## 15.4 Matrix Analysis

The single-particle decay scenario discussed above can be discussed efficiently in terms of semi-unitary matrices.

**Definition 15.1** A semi-unitary matrix  $M$  is an  $m \times n$  complex matrix such that  $M^\dagger M = I_n$ , where  $I_n$  is the  $n \times n$  identity matrix.

**Exercise 15.2** Prove that no semi-unitary matrix exists if  $m < n$ .

Consider the  $X$  decay scenario discussed above. If the initial labstate  $\Psi_0$  is represented by the  $1 \times 1$  column vector  $[\Psi_0] \equiv [1]$ , then the action of  $U_{1,0}$  acting on that labstate  $\Psi_0$  given by (15.1) may be represented by the action of the  $2 \times 1$  semi-unitary matrix  $U_{1,0} \equiv \begin{bmatrix} \alpha \\ \beta \end{bmatrix}$  acting on  $[\Psi_0]$ , giving

$$[\Psi_1] \equiv U_{1,0}[\Psi_0] = \begin{bmatrix} \alpha \\ \beta \end{bmatrix} [1] = \begin{bmatrix} \alpha \\ \beta \end{bmatrix}. \quad (15.15)$$

The two required transition amplitudes at stage  $\Sigma_1$  are just the two components of this vector.

Continuing this process to the next stage, we deduce that the labstate  $[\Psi_2]$  at stage  $\Sigma_2$  is represented by the action of the semi-unitary matrix  $U_{2,1} \equiv \begin{bmatrix} \alpha & 0 \\ \beta & 0 \\ 0 & 1 \end{bmatrix}$  on  $[\Psi_1]$ , giving

$$[\Psi_2] \equiv U_{2,1}[\Psi_1] = \begin{bmatrix} \alpha & 0 \\ \beta & 0 \\ 0 & 1 \end{bmatrix} \begin{bmatrix} \alpha \\ \beta \end{bmatrix} = \begin{bmatrix} \alpha^2 \\ \alpha\beta \\ \beta \end{bmatrix}. \quad (15.16)$$

For  $n > 1$ , the relevant semi-unitary matrix is an  $(n+1) \times n$  matrix given by

$$U_{n+1,n} = \begin{bmatrix} \alpha & \boldsymbol{\theta}_{n-1}^T \\ \beta & \boldsymbol{\theta}_{n-1}^T \\ \boldsymbol{\theta}_{n-1} & I_{n-1} \end{bmatrix}, \quad (15.17)$$

where  $\boldsymbol{\theta}_n$  is a column of  $n$  zeros,  $\boldsymbol{\theta}_n^T$  is its transpose, and  $I_n$  is the  $n \times n$  identity matrix. This leads to the final state  $[\Psi_n]$  at stage  $\Sigma_n$ :

$$[\Psi_n] = U_{n,n-1}U_{n-1,n-2} \dots U_{1,0}[\Psi_0] = \begin{bmatrix} \alpha^n \\ \beta\alpha^{n-1} \\ \vdots \\ \beta\alpha \\ \beta \end{bmatrix}. \quad (15.18)$$

The squared modulus of the first component of this column vector gives the same survival probability  $|\alpha|^{2n}$  as before. It is also easy to read off all the other transition amplitudes and from them determine discrete time versions of the  $P$ ,  $Q$ , and  $R$  functions discussed by MS (Misra and Sudarshan, 1977).

Although the QDN analysis gives results that look formally like the standard decay result, the scenario involved is equivalent to that discussed by MS; namely, there is a constant questioning (or its discrete equivalent) by the apparatus as to whether decay has taken place or not. In this case the results are simple. For Kaon and B meson decays, the results are more complicated.

### 15.5 The Ammonium System

In order to understand the QDN approach to neutral Kaon decay, discussed in the next section, it will be necessary to review first how stable systems such as the ammonium molecule are dealt with in our formalism.

The ammonium molecule consists of three hydrogen atoms and one nitrogen atom. If we ignore molecular rotation and translation as inessential to this argument, then we can think of the three hydrogen atoms as defining a plane in three dimensions. Then the nitrogen can be found on either side of this plane. What is observed is consistent with the classical explanation that the nitrogen oscillates from one side of this plane to the other and back with a characteristic frequency. It is this behavior that is the focus of our discussion here.

#### The Standard QM Account

With the above assumptions about neglecting rotation and translation, a simple but effective model of the ammonium molecule is described quantum mechanically as a superposition of two orthonormal states,  $|X\rangle$  and  $|Y\rangle$ , each of which represents one of the two possible position states of the single nitrogen atom relative to the plane defined by the three hydrogen atoms. These two states form a basis for a two-dimensional Hilbert space  $\mathcal{H}_{AM}$ , in other words, a qubit. It is interesting to note that we have encountered here a naturally occurring preferred basis for a qubit, that is, one that is dictated not by detector apparatus but by the assumed geometry of the SUO.

An account of the nonrelativistic quantum theory for ammonium is given by Feynman et al. (1966) so we give only a simplified brief resume here to set the scene.

It is most convenient to use a matrix representation for the states and the Hamiltonian operator. We define the preferred basis representation

$$|X\rangle \underset{R}{=} \begin{bmatrix} 1 \\ 0 \end{bmatrix}, \quad |Y\rangle \underset{R}{=} \begin{bmatrix} 0 \\ 1 \end{bmatrix}. \quad (15.19)$$

Then relative to this representation, the Hamiltonian for the system is given by the Hermitian matrix

$$H \underset{R}{=} \begin{bmatrix} e & f \\ f^* & e \end{bmatrix}, \quad (15.20)$$

where  $e$  is real and  $f$  can be complex. When  $f$  is zero, the two states are degenerate energy eigenstates and so are stable. This possibility is of no interest here, so we shall assume that  $f = |f|e^{i\phi}$ , where  $|f|$  is nonzero and  $\phi$  is a constant phase.

The two eigenvalues of  $H$  are  $E^\pm \equiv e \pm |f|$  with corresponding normalized energy eigenstates

$$|\pm\rangle \underset{R}{=} \frac{1}{\sqrt{2}} \begin{bmatrix} e^{i\phi} \\ \pm 1 \end{bmatrix}, \quad (15.21)$$

where we have set the arbitrary phases to zero for convenience. Hence an arbitrary normalized solution to the Schrödinger equation

$$i\hbar \frac{d}{dt} |\Psi, t\rangle = H |\Psi, t\rangle \tag{15.22}$$

has matrix representation

$$|\Psi, t\rangle \underset{R}{=} ae^{-iE^+t/\hbar} |+\rangle + be^{-iE^-t/\hbar} |-\rangle, \tag{15.23}$$

where  $|a|^2 + |b|^2 = 1$ .

If now we calculate the probability  $\text{Pr}(X, t|\Psi, 0) \equiv \langle X|\Psi, t\rangle$  that the SUO be found in state  $|X\rangle$  at time  $t > 0$  we find

$$\text{Pr}(X, t|\Psi, 0) = \frac{1}{2} + |ab| \cos(\beta - \alpha + 2|f|t/\hbar), \tag{15.24}$$

where  $a = |a|e^{i\alpha}$ ,  $b = |b|e^{i\beta}$ . Similarly, we find

$$\text{Pr}(Y, t|\Psi, 0) = \frac{1}{2} - |ab| \cos(\beta - \alpha + 2|f|t/\hbar). \tag{15.25}$$

These probabilities successfully model our expectations. First, if  $f$  is zero, then these probabilities are fixed. Second, if the initial state is prepared in an energy eigenstate to begin with, which means setting either  $a$  or  $b$  to zero, then the probability of finding the SUO in state  $|X\rangle$  is the same as that of finding it in state  $|Y\rangle$ .

**The QDN Account**

In the QDN description, the temporal architecture is given by Figure 15.2. It is assumed that there are two different detectable signal states,  $X, Y$ , with signal operators  $\hat{A}_n^X, \hat{A}_n^Y$ , respectively, evolving from stage  $\Sigma_n$  to stage  $\Sigma_{n+1}$  according to the rule

$$\begin{aligned} \mathbb{U}_{n+1,n} \hat{A}_n^X \mathbf{0}_n &= \{A \hat{A}_{n+1}^X + B \hat{A}_{n+1}^Y\} \mathbf{0}_{n+1}, \\ \mathbb{U}_{n+1,n} \hat{A}_n^Y \mathbf{0}_n &= \{C \hat{A}_{n+1}^X + D \hat{A}_{n+1}^Y\} \mathbf{0}_{n+1}, \end{aligned} \tag{15.26}$$

where  $\mathbb{U}_{n+1,n}$  is a semi-unitary operator and  $A, B, C$ , and  $D$  are constants determined by the dynamics of the situation. Semi-unitarity requires the constraints

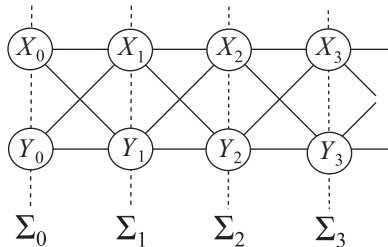


Figure 15.2. The temporal architecture of the ammonium molecule, with the two orthogonal states denoted  $X$  and  $Y$ .

$|A|^2 + |B|^2 = |C|^2 + |D|^2 = 1, A^*C + B^*D = 0$ , which is equivalent to standard unitarity in quantum mechanics in this case, because the rank of the quantum register is constant from stage to stage. All other states will be disregarded on the basis that there are no dynamical channels between them and states  $X, Y$ .

From (15.26) we can find a dyadic representation for  $\mathbb{U}_{n+1,n}$  in the form

$$\mathbb{U}_{n+1,n} = \Phi_{n+1}^T U \overline{\Phi}_n, \tag{15.27}$$

where

$$\Phi_{n+1}^T \equiv [\widehat{\mathbb{A}}_{n+1}^X \mathbf{0}_{n+1}, \widehat{\mathbb{A}}_{n+1}^Y \mathbf{0}_{n+1}], \quad \overline{\Phi}_n \equiv \begin{bmatrix} \overline{\mathbf{0}_n \mathbb{A}_n^X} \\ \overline{\mathbf{0}_n \mathbb{A}_n^Y} \end{bmatrix}, \tag{15.28}$$

and  $U$  is the unitary matrix

$$U \equiv \begin{bmatrix} A & C \\ B & D \end{bmatrix}. \tag{15.29}$$

The retraction  $\overline{\mathbb{U}_{n+1,n}}$  of  $\mathbb{U}_{n+1,n}$  is given by

$$\overline{\mathbb{U}_{n+1,n}} = \Phi_n^T U^\dagger \overline{\Phi}_{n+1} \tag{15.30}$$

and satisfies the relation  $\overline{\mathbb{U}_{n+1,n}} \mathbb{U}_{n+1,n} = \mathbb{I}_n^c$ , where  $\mathbb{I}_n^c$  is the contextual identity operator

$$\mathbb{I}_n^c \equiv \widehat{\mathbb{A}}_n^X \mathbf{0}_n \overline{\mathbf{0}_n \mathbb{A}_n^X} + \widehat{\mathbb{A}}_n^Y \mathbf{0}_n \overline{\mathbf{0}_n \mathbb{A}_n^Y} \tag{15.31}$$

for the contextual subspace  $\mathcal{Q}_n^c$  with orthonormal basis  $\{\widehat{\mathbb{A}}_n^X \mathbf{0}_n, \widehat{\mathbb{A}}_n^Y \mathbf{0}_n\}$ .

The form (15.27) is particularly suitable for finding the evolution operator  $\mathbb{U}_{N,0}$  taking states of the SUO from stage  $\Sigma_0$  to some final stage  $\Sigma_N$ . We find

$$\mathbb{U}_{N,0} = \Phi_N^T U^N \overline{\Phi}_0, \quad N = 0, 1, 2, \dots \tag{15.32}$$

The problem therefore reduces to finding  $U^N$ , which we do as follows.

As discussed in Section 11.5, a unitary matrix  $U$  such as (15.29) can always be put in standard form, that is,

$$U = e^{i\eta} \begin{bmatrix} a & -b^* \\ b & a^* \end{bmatrix}, \tag{15.33}$$

where  $\eta$  is real and  $a$  and  $b$  satisfy the condition  $|a|^2 + |b|^2 = 1$ .

**Exercise 15.3** Find expressions for  $\eta, a$ , and  $b$  in terms of  $A, B, C$ , and  $D$ .

We now state without proof that matrix  $U$  can be written in the form

$$U = e^{i\eta} V \Lambda V^\dagger, \tag{15.34}$$

where matrix  $V$  is a unitary matrix given by

$$V \equiv \begin{bmatrix} u & -v^* \\ v & u^* \end{bmatrix}, \tag{15.35}$$

where  $|u|^2 + |v|^2 = 1$  and  $\Lambda$  is the diagonal matrix

$$\Lambda \equiv \begin{bmatrix} \lambda^+ & 0 \\ 0 & \lambda^- \end{bmatrix}. \quad (15.36)$$

Here  $\lambda^+$ ,  $\lambda^-$  are the two eigenvalues of  $U$  and so are the roots of the equation  $\lambda^2 - (a + a^*)\lambda + 1 = 0$ . These roots are complex conjugates of each other and have magnitude one, so we can write  $\lambda^+ = e^{i\theta}$ ,  $\lambda^- = e^{-i\theta}$  for some real angle  $\theta$ . The relations between  $u, v$  and  $a, b$  are

$$a = |u|^2 e^{i\theta} + |v|^2 e^{-i\theta}, \quad b = u^* v (e^{i\theta} - e^{-i\theta}), \quad (15.37)$$

noting that these are nonlinear in  $u$  and  $v$ . Indeed,  $u$  and  $v$  are not unique: we can multiply each by an element of the unit circle without changing relations (15.37).

The significance of the form (15.34) is that it is now easy to evaluate powers of  $U$ . Specifically, we find

$$\mathbb{U}_{n,0} = e^{in\theta} \Phi_n^T V \Lambda^n V^\dagger \overline{\Phi}_0. \quad (15.38)$$

Applying this to the evolution of the signal operators then gives, modulo a phase factor,

$$\begin{aligned} \widehat{\mathbb{A}}_0^X &\rightarrow \{|u|^2 e^{in\theta} + |v|^2 e^{-in\theta}\} \widehat{\mathbb{A}}_n^X + u^* v \{e^{in\theta} - e^{-in\theta}\} \widehat{\mathbb{A}}_n^Y, \\ \widehat{\mathbb{A}}_0^Y &\rightarrow uv^* \{e^{in\theta} - e^{-in\theta}\} \widehat{\mathbb{A}}_n^X + \{|u|^2 e^{-in\theta} + |v|^2 e^{in\theta}\} \widehat{\mathbb{A}}_n^Y. \end{aligned} \quad (15.39)$$

Hence we find the conditional probabilities

$$\begin{aligned} \Pr(X, n|X, 0) &= \Pr(Y, n|Y, 0) = |u|^4 + |v|^4 + 2|u|^2|v|^2 \cos(2n\theta), \\ \Pr(Y, n|X, 0) &= \Pr(X, n|Y, 0) = 4|u|^2|v|^2 \sin^2(n\theta), \end{aligned} \quad (15.40)$$

which agrees with the QM expressions (15.24) and (15.25) when the parameters  $u, v$ , and  $\theta$  are chosen suitably.

It was noted by Itano et al. (1990) that a survival probability of the form  $P(\tau) \sim 1 - \gamma\tau^2 + O(\tau^3)$  would be needed to make observations of the quantum Zeno effect viable. The above calculation of the ammonium survival probabilities is compatible with this, as can be seen from the expansion

$$\begin{aligned} \Pr(X, n|X, 0) &= |u|^4 + |v|^4 + 2|u|^2|v|^2 \cos(2n\theta) \\ &\sim 1 - 4|u|^2|v|^2 n^2 \theta^2 + O(n^4 \theta^4). \end{aligned} \quad (15.41)$$

Therefore, it is predicted that the quantum Zeno effect (or at least behavior analogous to it) should be observable in the ammonium system, if the right experimental conditions are set up. As with the particle decays discussed in the previous section, it would be necessary to ensure that the two limits,  $t \rightarrow \infty$ ,  $\tau \rightarrow 0$ , were carefully balanced.

## 15.6 Kaon-type Decays

The explanation by Gell-Mann and Pais (Gell-Mann and Pais, 1955) of the phenomenon of regeneration in neutral Kaon decay was a successful application of

QM to particle physics. In the standard calculation (Feynman et al., 1966), a non-Hermitian Hamiltonian is used to introduce the two decay parameters needed to describe the observations. We will show that QDN readily reproduces the results of the Gell-Mann and Pais calculation while conserving total probability and without the introduction of any complex energies.

The analysis of the Kaon system is more complicated than the single-particle decay process discussed above, involving the interplay of two distinct neutral Kaons, the  $K^0$  and its antiparticle, the  $\bar{K}^0$ . In that respect, our discussion in the previous section of the ammonium molecule is useful. The QDN discussion of neutral Kaon decay goes as follows (Jaroszkiewicz, 2008b).

Consider three different particle states,  $X, Y$ , and  $Z$ , making transitions between each other in the specific way described below. An important example of such behavior in particle physics involves the neutral Kaons, with  $X$  representing a  $K^0$  meson,  $Y$  representing a  $\bar{K}^0$  meson, and  $Z$  representing their various decay products. Kaon decay is remarkable for the phenomenon of regeneration, in which the Kaon survival probabilities fall and then rise with time. A similar phenomenon has been observed in  $B$  meson decay (Karyotakis and de Monchenault, 2002).

As before, attention can be restricted to signality-one states. The dynamics is described by the transition rules

$$\widehat{A}_n^X \rightarrow \alpha \widehat{A}_{n+1}^X + \beta \widehat{A}_{n+1}^Y + \gamma \widehat{A}_{n+1}^{Z^{n+1}}, \tag{15.42}$$

$$\widehat{A}_n^Y \rightarrow u \widehat{A}_{n+1}^X + v \widehat{A}_{n+1}^Y + w \widehat{A}_{n+1}^{Z^{n+1}}, \tag{15.43}$$

$$\widehat{A}_n^{Z^a} \rightarrow \widehat{A}_{n+1}^{Z^a}, \quad a = 1, 2, \dots, n \tag{15.44}$$

where semi-unitarity requires the transition coefficients to satisfy the constraints

$$|\alpha|^2 + |\beta|^2 + |\gamma|^2 = |u|^2 + |v|^2 + |w|^2 = 1, \quad \alpha^*u + \beta^*v + \gamma^*w = 0. \tag{15.45}$$

The above process is a combination of the decay and oscillation processes discussed in previous sections.

The temporal architecture is given by Figure 15.3: the dynamics given by (15.42)–(15.44) rules out transitions from  $Z$  states to either  $X$  or  $Y$  states. Therefore, once a  $Z$  state is created, it remains a  $Z$  state, so there is an irreversible

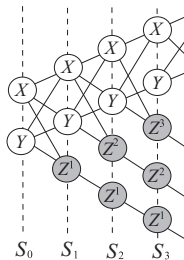


Figure 15.3. The temporal architecture of Kaon decay.

flow from the  $X$  and  $Y$  states and so these eventually disappear. Before that occurs, however, there will be back-and-forth transitions between the  $X$  and  $Y$  states that give rise to the phenomenon of regeneration.

In actual Kaon decay experiments, pure  $K^0$  states can be prepared via the strong interaction process  $\pi^- + p \rightarrow K^0 + \Lambda$ , while pure  $\bar{K}^0$  states can be prepared via the process  $\pi^+ + p \rightarrow K^+ + \bar{K}^0 + p$ . In our notation, these preparations correspond to initial labstates  $\hat{\mathbb{A}}_0^X \mathbf{0}_n$  and  $\hat{\mathbb{A}}_0^Y \mathbf{0}_0$ , respectively. In practice, superpositions of  $K^0$  and  $\bar{K}^0$  states may be difficult to prepare directly, but the analysis of Gell-Mann and Pais shows that such states could in principle be prepared indirectly (Gell-Mann and Pais, 1955). Therefore, labstates corresponding to  $X$  and  $Y$  superpositions are physically meaningful and will be used in the following analysis.

Consider an initial labstate of the form  $\Psi_0 \equiv \{x_0 \hat{\mathbb{A}}_0^X + y_0 \hat{\mathbb{A}}_0^Y\} \mathbf{0}_0$ , where  $|x_0|^2 + |y_0|^2 = 1$ . Matrix methods are appropriate here. The dynamics of the system will be discussed in terms of the initial column vector  $\underline{\Psi}_0 \equiv [x_0 \ y_0]^T$ , equivalent to the statement that each run of the experiment starts with the rank-two lab register  $\mathcal{Q}_0 \equiv Q_0^X Q_0^Y$ . The dynamical rules (15.42)–(15.44) map labstates in  $\mathcal{Q}_0$  into  $\mathcal{Q}_1 \equiv Q_1^X Q_1^Y Q_1^{Z^1}$ , so there is a change of rank from two to three. The transition is represented by the semi-unitary matrix

$$U_{1,0} \equiv \begin{bmatrix} \alpha & u \\ \beta & v \\ \gamma & w \end{bmatrix}, \tag{15.46}$$

which subsequently generalizes to

$$U_{n+1,n} \equiv \begin{bmatrix} \alpha & u & \underline{0}_n^T \\ \beta & v & \underline{0}_n^T \\ \gamma & w & \underline{0}_n^T \\ \underline{0}_n & \underline{0}_n & I_n \end{bmatrix}, \quad n > 0, \tag{15.47}$$

where  $I_n$  is the  $n \times n$  identity matrix and  $\underline{0}_n$  is a column of  $n$  zeros. The observer’s detector array increases rank by one over each time step. The state at stage  $\Sigma_n$  is represented by a column vector  $\underline{\Psi}_n$  with  $n + 2$  components, given by  $\underline{\Psi}_n = U_{n,n-1} U_{n-1,n-2} \dots U_{2,1} U_{1,0} \underline{\Psi}_0$ . Overall probability is conserved, because of the semi-unitarity of the transition operators.

As before, the key to unraveling the dynamics is linearity, which is guaranteed by the use of semi-unitary evolution operators. Suppose the state  $\underline{\Psi}_n$  at time  $n$  is represented by

$$\underline{\Psi}_n = [x_n, y_n, z_n^n, \dots, z_n^1]^T, \tag{15.48}$$

where the components  $x_n$  and  $y_n$  are such that  $x_n = \lambda^n x_0$  and  $y_n = \lambda^n y_0$ , where  $\lambda$  is some complex number to be determined. Such states will be referred to as *eigenmodes*. They are not eigenstates of any physical operator, but their first two

components,  $x_n$  and  $y_n$ , behave as if they were. The dynamics gives the relations  $x_{n+1} = \alpha x_n + u y_n = \lambda x_n$ ,  $y_{n+1} = \beta x_n + v y_n = \lambda y_n$ , and  $z_{n+1}^{n+1} = \gamma x_n + w y_n$ .

Experimentalists will be interested principally in survival probabilities for the  $X$  and  $Y$  states, so the dynamics of  $Z$  states will be ignored here; i.e., the behavior of the components  $z_n^k$  for  $k < n$  will not be discussed. Clearly, however, the QDN formalism is capable of giving much more specific details about the process than just the  $X$  and  $Y$  survival probabilities.

It will be seen from the above that  $\lambda$  is an eigenvalue of the matrix

$$\begin{bmatrix} \alpha & u \\ \beta & v \end{bmatrix},$$

which means that in principle there are two solutions,  $\lambda^+$  and  $\lambda^-$ , for the eigenmode values, given by  $\lambda^\pm = \frac{1}{2}\{\alpha + v \pm \sqrt{(\alpha - v)^2 + 4\beta u}\}$ . It is expected that these will not be mutual complex conjugates in actual experiments, because if they were, the analysis could not explain observed Kaon physics. Therefore, the coefficients  $\alpha$ ,  $\beta$ ,  $u$ , and  $v$  will be such that the above two eigenmode values are complex and of different magnitude and phase, giving rise to two decay channels with different lifetimes, as happens in neutral Kaon decay. In the quantum mechanics analysis of neutral Kaon decays, Gell-Mann and Pais described the neutral Kaons as superpositions of two hypothetical particles known as  $K_1^0$  and  $K_2^0$ , which are charge-parity eigenstates and have different decay lifetimes (Gell-Mann and Pais, 1955). The  $K_1^0$  decays to a two-pion state with a lifetime of about  $0.9 \times 10^{-10}$  second, while the  $K_2^0$  decays to a three-pion state with a lifetime of about  $0.5 \times 10^{-7}$  second.

Semi-unitarity guarantees that

$$|x_{n+1}|^2 + |y_{n+1}|^2 + |z_{n+1}^{n+1}|^2 = |x_n|^2 + |y_n|^2, \tag{15.49}$$

and so it can be deduced that

$$|\lambda|^2 = 1 - \frac{|z_{n+1}^{n+1}|^2}{|x_n|^2 + |y_n|^2} < 1, \quad n = 0, 1, 2, \dots, \tag{15.50}$$

given  $|x_n|^2 + |y_n|^2 > 0$ . From this and the conditions  $x_n = \lambda^n x_0$ ,  $y_n = \lambda^n y_0$ , the eigenmode values can be written in the form  $\lambda_1 \equiv \lambda^+ = \rho_1 e^{i\theta_1}$ ,  $\lambda_2 \equiv \lambda^- = \rho_2 e^{i\theta_2}$ , where  $0 < \rho_1, \rho_2 < 1$  and  $\theta_1$  and  $\theta_2$  are real. The eigenmodes at time  $t = 0$  corresponding to  $\lambda_1$  and  $\lambda_2$  will be denoted by  $\underline{\Lambda}_{1,0}$  and  $\underline{\Lambda}_{2,0}$  respectively, i.e.  $\underline{\Lambda}_{1,0} = [ a_1 \quad b_1 ]^T$ ,  $\underline{\Lambda}_{2,0} = [ a_2 \quad b_2 ]^T$ , and then the evolution rules give

$$\underline{\Lambda}_{1,n} = \begin{bmatrix} \lambda_1^n a_1 \\ \lambda_1^n b_1 \\ c_{n,n} \\ \vdots \\ c_{1,n} \end{bmatrix}, \quad \underline{\Lambda}_{2,n} = \begin{bmatrix} \lambda_2^n a_2 \\ \lambda_2^n b_2 \\ d_{n,n} \\ \vdots \\ d_{1,n} \end{bmatrix}, \tag{15.51}$$

where the coefficients  $\{c_{k,n}\}, \{d_{k,n}\}$  can be determined from the dynamics. The initial modes  $\underline{\Lambda}_{1,0}$  and  $\underline{\Lambda}_{2,0}$  are linearly independent provided  $\lambda_1$  and  $\lambda_2$  are different. Given that, then any initial labstate  $\underline{\Psi}_0$  can be expressed uniquely as a normalized linear combination of  $\underline{\Lambda}_{1,0}$  and  $\underline{\Lambda}_{2,0}$ , i.e.,  $\underline{\Psi}_0 = \mu_1 \underline{\Lambda}_{1,0} + \mu_2 \underline{\Lambda}_{2,0}$ , for some coefficients  $\mu_1$  and  $\mu_2$ . This is the analogue of the decompositions

$$\begin{aligned} |K^0\rangle &= \{|K_1^0\rangle + |K_2^0\rangle\}/\sqrt{2}, \\ |\bar{K}^0\rangle &= \{|K_1^0\rangle - |K_2^0\rangle\}/\sqrt{2} \end{aligned} \quad (15.52)$$

in the Gell-Mann and Pais approach.

From this, the amplitude  $\mathcal{A}(X, n|\Psi, 0)$  to find an  $X$  signal at time  $n$  is given by

$$\mathcal{A}(X, n|\Psi, 0) = \mu_1 a_1 \lambda_1^n + \mu_2 a_2 \lambda_2^n, \quad (15.53)$$

so that the survival probability for  $X$  is given by

$$\begin{aligned} \text{Pr}(X, n|\Psi, 0) &= |\mu_1|^2 |a_1|^2 \rho_1^{2n} + |\mu_2|^2 |a_2|^2 \rho_2^{2n} \\ &\quad + 2\rho_1^n \rho_2^n \text{Re}\{\mu_1^* \mu_2 a_1^* a_2 e^{-i(\theta_1 - \theta_2)}\}, \end{aligned} \quad (15.54)$$

and similarly for  $\text{Pr}(Y, n|\Psi, 0)$ .

There is scope here for various limits to be considered, as discussed in the single-channel decay analysis, such that either particle decay is seen or the quantum Zeno effect appears to hold over limited time spans. If we are justified on empirical grounds in writing  $\rho_1^n \equiv e^{-\Gamma_1 t/2}$ ,  $\rho_2^n \equiv e^{-\Gamma_2 t/2}$ , where  $t \equiv n\tau$  and  $\Gamma_1, \Gamma_2$  correspond to long and short lifetime decay parameters, respectively, then the various constants can always be chosen to get full agreement with the standard Kaon survival intensity functions

$$\begin{aligned} I(K^0) &= (e^{-\Gamma_1 t} + e^{-\Gamma_2 t} + 2e^{-(\Gamma_1 + \Gamma_2)t/2} \cos \Delta m t)/4, \\ I(\bar{K}^0) &= (e^{-\Gamma_1 t} + e^{-\Gamma_2 t} - 2e^{-(\Gamma_1 + \Gamma_2)t/2} \cos \Delta m t)/4, \end{aligned} \quad (15.55)$$

for pure  $K^0$  decays. Here  $\Delta m$  is proportional to the proposed mass difference between the hypothetical  $K_1^0$  and  $K_2^0$  “particles,” which are each charge-parity eigenstates and are supposed to have charge-parity-conserving decay channels. From the QDN approach, such objects need not exist. Instead, they are regarded as manifestations of different possible superpositions of  $K^0$  and  $\bar{K}^0$  labstates, each of which is physically realizable via the strong interactions, as mentioned above. Conversely, the apparatus dynamics may be such that quantum Zeno-type effects are observed instead of long-term decays. Again, this will depend on the details of the experiment chosen.